

# Characterization of Medicinal Compounds Confined in Porous Media by Neutron Vibrational Spectroscopy and First-Principles Calculations: A Case Study with Ibuprofen

Ken K. Qian · Wei Zhou · Xiaoming Xu · Terrence J. Udovic

Received: 13 December 2011 / Accepted: 30 April 2012 / Published online: 15 May 2012  
© Springer Science+Business Media, LLC 2012

## ABSTRACT

**Purpose** Amorphous formulations of ibuprofen were prepared by confining the drug molecules into the porous scaffolds. The molecular interactions between ibuprofen and porous media were investigated using neutron vibrational spectroscopy.

**Methods** Ibuprofen was introduced into the pores using sublimation and adsorption method. Neutron vibrational spectra of both neat and confined ibuprofen were measured, and compared to the simulated ibuprofen spectra using first-principles phonon calculations.

**Results** The neutron vibrational spectra showed marked difference between the neat crystalline and the confined ibuprofen in low-frequency region, indicating a loss of the overall structural order once the ibuprofen molecules were in the pores. Furthermore, the formation of ibuprofen dimers, which is found in the crystal structure, was greatly inhibited, possibly due to the preferential interactions between the carboxylic acid group of ibuprofen ( $-\text{COOH}$ ) and the surface hydroxyl groups of porous scaffolds ( $\text{Si-OH}$ ).

**Conclusions** The experimental evidence suggests that, at the current drug loading, most, if not all, of the confined ibuprofen molecules were bound to the pore surfaces via hydrogen bonding. The structural arrangement of ibuprofen in the pores appears to be monolayer coverage. In addition, neutron vibrational spectroscopy is proven an exceedingly useful technique to study adsorbent-adsorbate interactions.

**KEY WORDS** amorphization · first-principles calculations · mesoporous · neutron vibrational spectroscopy · silicon dioxide

## INTRODUCTION

Amorphous solids are of significant interest in pharmaceutical research and development (1,2). A drug in an amorphous state has enhanced aqueous solubility and dissolution rate in comparison to its corresponding crystalline phase. However, an amorphous solid, being in a higher free energy state, can crystallize to a thermodynamically more stable form, thus offsetting the benefits of amorphization. In recent studies, a unique amorphization technique utilizing mesoporous materials (3), with mean pore diameters between 2 nm and 50 nm, has been reported (4–8). Striking observations were made that crystalline compounds, such as ibuprofen, became amorphous spontaneously after they were physically mixed with mesoporous silicon dioxide ( $\text{SiO}_2$ ) and stored. Using powder X-ray diffraction (PXRD), the phase transformation was evidenced by the gradual disappearance of Bragg peaks over time. The pathway of the amorphization was found to occur via the vapor phase, i.e., sublimation of the crystals, followed by sorption of the molecules into the porous scaffolds (6,7). Significant improvements in the rate and extent of drug release due to competitive adsorption were also witnessed (8). Once this amorphous system was dispersed in an aqueous medium, water molecules preferentially interacted with the surface of porous media by displacing the adsorbed drug molecules, which resulted in a supersaturated solution. Given that an increasing number of drug molecules in the pharmaceutical industry pipeline are poorly soluble in aqueous media, this technique can be a new strategy in solubility enhancement. Successful product development, therefore, requires a

K. K. Qian (✉) · W. Zhou · T. J. Udovic  
National Institute of Standards and Technology (NIST)  
NIST Center for Neutron Research (NCNR)  
100 Bureau Drive  
Gaithersburg, Maryland 20899, USA  
e-mail: ken.qian@nist.gov

X. Xu  
Department of Pharmaceutical Sciences, School of Pharmacy  
University of Connecticut  
69 North Eagleville Road, Unit 3092  
Storrs, Connecticut 06269, USA

thorough knowledge of this amorphous system, such as the drug-porous media interactions.

Properties of drug molecules under confinement are markedly different than those in the bulk phases, the phenomena of which are not well understood (9). For example, Mellaerts *et al.* studied the physical state of ibuprofen encapsulated in porous SiO<sub>2</sub>, SBA-15, with 8.4-nm pores using differential scanning calorimetry (10). Ibuprofen was introduced into SBA-15 by incipient wetness impregnation, solution-state adsorption, or melt infiltration to achieve 20 % and 30 % (by mass) drug loading. The composites containing 20 % ibuprofen, prepared by the three methods, showed broad signals at -43°C, which were attributed to possible glass transitions of ibuprofen in the pores. However, as the temperature was increased, thermal transitions were observed, but could not be clearly defined due to the severely shifted baselines and very broad signals. At 30 % drug loading, similar behavior was recorded, with the exception of SBA-15-ibuprofen prepared using the incipient wetness impregnation method. A melting endotherm at 76°C, which corresponds to the bulk melting point of ibuprofen, was clearly detected. Although the adsorption of ibuprofen on the surface of SBA-15 was considered the primary interaction mechanism, a satisfactory explanation regarding the conflicting observations, i.e., prominent bulk properties of confined ibuprofen indicated by the thermal analyses, was not provided.

Others considered the mobility of confined medicinal compounds as surrogate to elucidate the interactions between guest molecules and porous scaffolds. For example, Bras *et al.* introduced ibuprofen into SBA-15 with 8.6-nm pores by solution-state adsorption to achieve 27 % (by mass) drug loading (11). Using dielectric relaxation spectroscopy, the authors observed two populations of ibuprofen with different mobilities. The molecules with slower dynamics were thought to adsorb on the pore walls, while the ones with faster dynamics were present in the center of the pores, forming dimers and trimers. However, since SBA-15 with only an ibuprofen monolayer was not prepared and analyzed as a reference, the conclusions appeared arbitrary.

The foregoing discussion illustrates the complex nature of interactions between confined molecules and porous media, which is further compounded by preparation methods and drug loadings. Although solvent infiltration is a useful method for producing amorphized drug infiltrates, many investigators use this technique to achieve high drug loadings without considering the amorphization capacity of porous materials. In particular, if the loadings exceed the volumetric pore capacity or the surface adsorption capacity of the porous scaffolds, any inadvertent crystallization, reflected in the bulk melting endotherm (10), and the formations of dimers and trimers (11), negates the purpose of amorphization. In contrast, when amorphization is realized via sublimation/adsorption, drug molecules are presumed to interact with the specific adsorption sites. The surfaces of SiO<sub>2</sub> have both siloxane

bridges (Si–O–Si) and hydroxyl (Si–OH or silanol) groups, the latter at an average density of 4.6 units/nm<sup>2</sup>, measured using the hydrogen-deuterium exchange method (12–14). These surface functional groups can form hydrogen bonds or other van der Waals types of interactions with guest molecules. The attainable adsorption or amorphization capacity, once reached, means that the system is in dynamic equilibrium. At this stage, further adsorption of drug molecules is precluded. Thus, this simpler model system, at or below the amorphization capacity, can be advantageous to elucidate the adsorbent-adsorbate interactions.

Herein, we investigate the interactions of confined ibuprofen with mesoporous materials using neutron vibrational spectroscopy (NVS). NVS has several advantages compared to optical vibrational techniques such as infrared or Raman spectroscopy. First, since photons are scattered by electrons, an infrared or Raman spectrum is generally more sensitive to vibrations of heavier atoms because of their larger electron densities (15). A typical mesoporous drug delivery system contains porous SiO<sub>2</sub> and a hydrogen-rich drug compound. In this case, photon scattering will be less sensitive to the drug compound, with signals predominantly from the porous media (e.g., Si). These drawbacks, however, can be circumvented using NVS. Because the neutron incoherent scattering cross-section of hydrogen is much greater than those of the common elements in a medicinal compound or porous material (Table I), spectra are dominated by the motion of hydrogen atoms present in the sample, making NVS better suited to analyze hydrogenous systems (16,17).

Second, NVS covers the molecular vibrational range of interest between 16 cm<sup>-1</sup> and 4000 cm<sup>-1</sup> with excellent resolution. The energy range below 400 cm<sup>-1</sup>, which is more difficult experimentally for infrared or Raman spectroscopy, is readily accessible by NVS. A third advantage of using NVS is that spectra are not subjected to optical selection rules. All vibrations are active and, in principle, measurable. It is thus more straightforward to predict the normal-mode vibrational intensities and frequencies by *ab initio* phonon calculations. The

**Table I** Neutron Incoherent Scattering Cross-Sections of Common Elements in Organic Compounds and Porous Media (Data Obtained from Ref. 17)

Element	Neutron Incoherent Scattering Cross-Section ( $\times 10^{-28}$ m <sup>2</sup> , or Barn)
Hydrogen (H)	80.27
Carbon (C)	0.001
Nitrogen (N)	0.50
Oxygen (O)	0.00
Magnesium (Mg)	0.08
Aluminum (Al)	0.0082
Silicon (Si)	0.004

calculated vibrational modes, complementary to the experimental spectra, can provide insights concerning the molecular interactions among drug molecules as well as between a drug molecule and its porous scaffold.

Therefore, the objective of the current study is to use NVS in conjunction with first-principles phonon calculations to characterize the interactions of a model compound, ibuprofen, with both mesoporous SiO<sub>2</sub> and magnesium aluminometasilicate (MAS). A better understanding on the molecular level will provide deeper insights on the disordered nature of confined drug molecules.

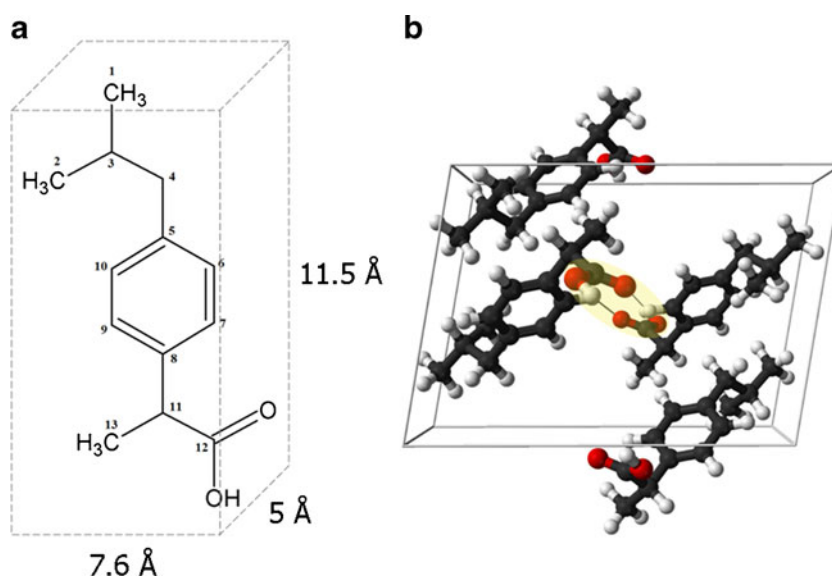
## MATERIALS AND METHODS

### Materials

All raw materials used in this investigation were from commercial sources (18). SiO<sub>2</sub> (Spherical silica gel, 62700) and MAS (Neusilin US2) were obtained from Sorbent Technologies (Atlanta, Georgia) and Fuji Chemical Industry Co. (Toyama, Japan), respectively. MAS has an empirical formula of Al<sub>2</sub>O<sub>3</sub> · MgO · 1.7 SiO<sub>2</sub> · n H<sub>2</sub>O. Crystalline ibuprofen (C<sub>13</sub>H<sub>18</sub>O<sub>2</sub>, United States Pharmacopeia grade) was obtained from Spectrum Chemicals (New Brunswick, New Jersey). Ibuprofen is a racemic mixture of S(+)-ibuprofen and R(-)-ibuprofen. Crystals exist as cyclic dimers, with one molecule in the S configuration and another in the R configuration forming double hydrogen bonds involving the carboxylic acid (-COOH) groups. The molecular structure and monoclinic unit cell of crystalline ibuprofen are shown in Fig. 1. The reported vapor pressure of ibuprofen is 1.7 × 10<sup>-2</sup> Pa at 40°C (19). The molecular dimensions of an ibuprofen molecule, when modeled as a rectangular prism, are 11.5 Å × 7.6 Å × 5 Å (20).

**Fig. 1** Ibuprofen (C<sub>13</sub>H<sub>18</sub>O<sub>2</sub>).

(a) Molecular structure with carbon atoms labeled. The approximate dimensions are obtained by modeling an ibuprofen molecule in a rectangular prism. (b) Monoclinic unit cell (C: black; O: red; H: white). Ibuprofen dimers form through the double hydrogen bonds involving the carboxylic acid groups.



Raw materials were passed through a 100-mesh screen to remove large particles and agglomerates. Both mesoporous media were dried in a vacuum oven (Lab-line, #3608-5, Barnstead International, Melrose Park, Illinois) at 110°C and 300 Pa (3 mbar) for 12 h to remove adsorbed moisture prior to use. All subsequent sample handling was performed in a glove box (Glove box series 100, Terra Universal, Fullerton, California) with a constant dry nitrogen purge at room temperature.

### Characterization of Bare Porous Materials

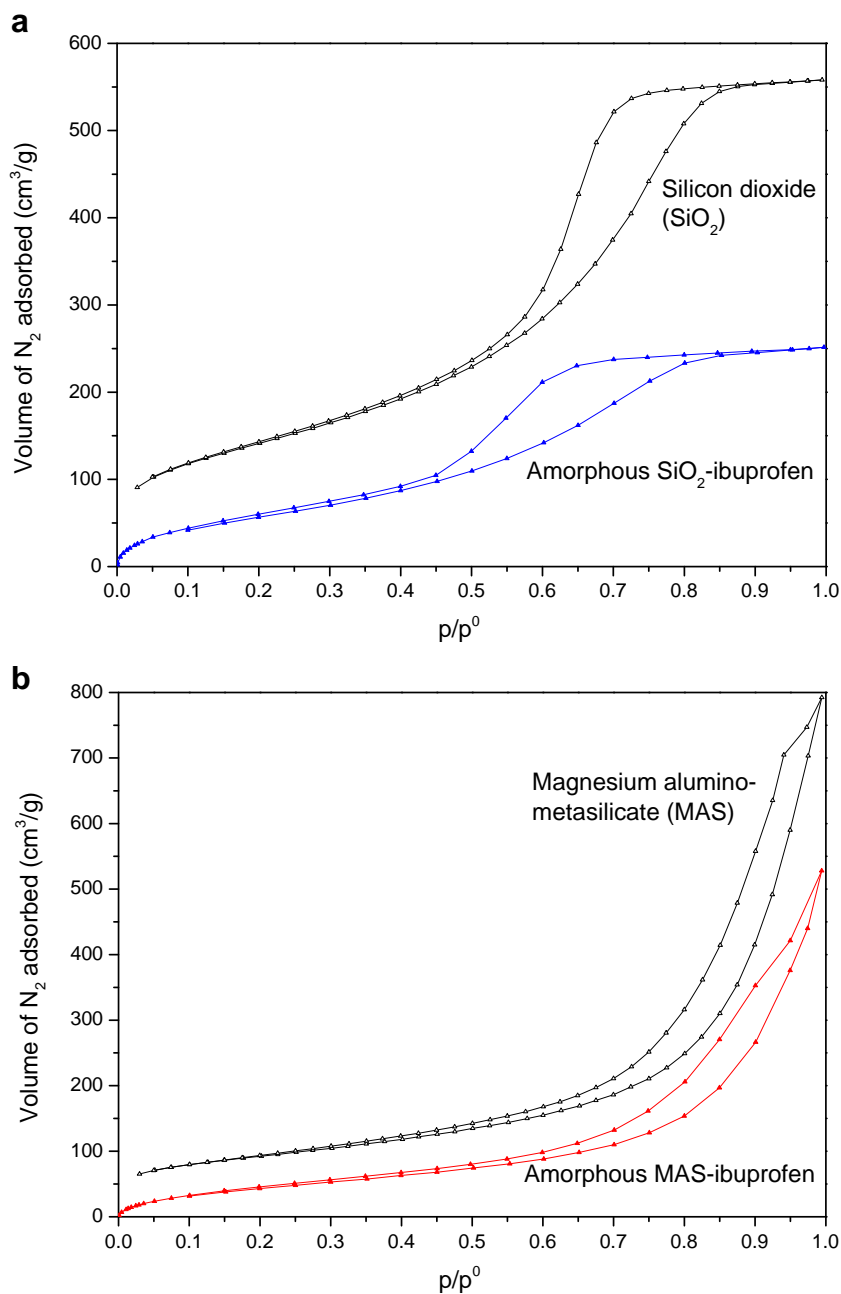
Surface areas, pore diameters and pore volumes of SiO<sub>2</sub> and MAS were determined using nitrogen adsorption/desorption (Autosorb-1, Quantachrome Instruments, Boynton Beach, Florida). After drying in a vacuum oven, a sample between 50 mg and 100 mg was weighed and used in each measurement. Specific surface areas (SSAs) were determined using the Brunauer-Emmett-Teller (BET) equation. Total pore volumes and pore size distributions were calculated by applying the Barrett-Joyner-Halenda (BJH) model to the desorption isotherm of nitrogen (21).

The porous structures of SiO<sub>2</sub> and MAS were further examined using small-angle X-ray scattering (SAXS) (Ultima III, Rigaku Corporation, Tokyo, Japan) with CuK $\alpha$  radiation at 40 kV and 40 mA ( $\lambda$ =1.54056 Å). Powders were tightly packed inside thin-walled quartz capillaries (outer diameter=1 mm, wall thickness=0.01 mm, capillary length=80 mm) (Charles Supper Company, Natick, Massachusetts). Samples were scanned from 0.1 ° to 3 ° at 0.05 °/min. After background corrections, the scattered intensity, I(q), was plotted as a function of scattering vector q. In the event of elastic scattering, the magnitude of q equals  $[4 \times \pi \times \sin(\theta)/\lambda]$ , where  $\theta$  is the Bragg angle or half of the scattering angle (in radian); and  $\lambda$  is the incident radiation wavelength.

## Preparation and Characterization of Physical Mixtures

Physical mixtures of porous media and ibuprofen at 3:1 mass ratios were weighed and gently mixed using a mortar and pestle to ensure content uniformity. The mixtures were then transferred to amber glass jars (diameter=5 cm, height=6.5 cm, volume=120 mL). The powder mixtures occupied approximately one-fifth of the container volume. The glass jars, with nitrogen in the headspace, were then sealed tightly with screw caps and placed in a lab desiccator. The desiccator was sealed and kept at 40°C in an oven (DKN 402, Yamato Scientific America, Santa Clara, California).

**Fig. 2** Nitrogen adsorption/desorption isotherms before and after the incorporation of ibuprofen. **(a)** Silicon dioxide ( $\text{SiO}_2$ ); **(b)** Magnesium aluminometasilicate (MAS).



The change in crystallinity of ibuprofen was monitored using PXRD (Ultima III, Rigaku Corporation, Tokyo, Japan) with  $\text{CuK}\alpha$  radiation at 40 kV and 40 mA. All samples were scanned from 5° to 50° at 1°/min. After the physical mixtures became amorphous, the changes in porous structure of the samples were again analyzed using nitrogen isotherms.

## Experimental Vibrational Spectra of Ibuprofen

The NVS measurements were performed using the BT-4 filter-analyzer neutron spectrometer (FANS) at the National Institute of Standards and Technology (NIST), NIST Center for Neutron Research (NCNR). FANS uses a Cu (220)

monochromator and 20 min of arc for both the pre- and post-monochromator horizontal collimations (22). These conditions provided full-width-at-half-maximum resolutions of 2 % to 4.5 % of the vibrational wavenumber over the range probed.

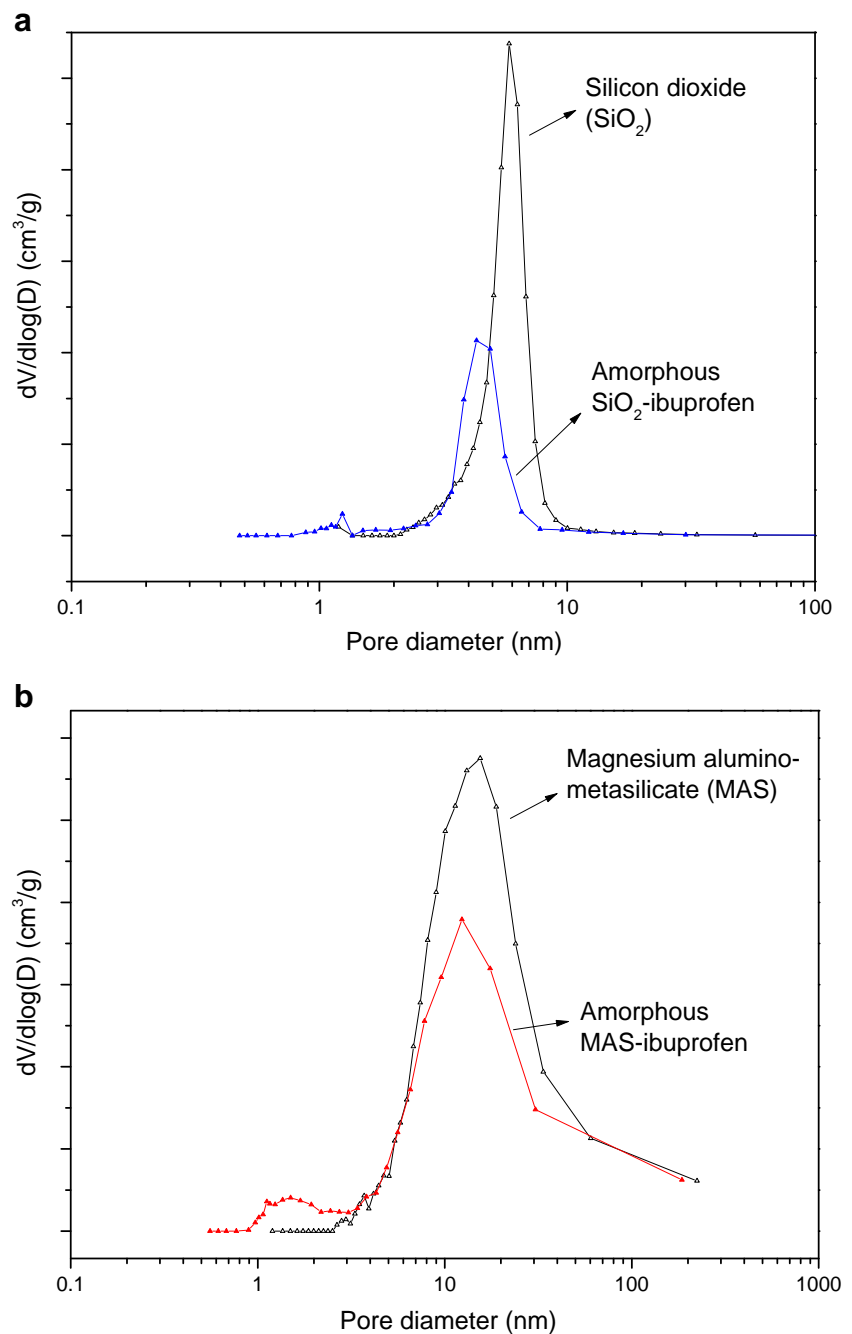
Powder samples, between 1 g and 5 g, were transferred to a cylindrical aluminum sample container and sealed with an indium o-ring. The container was then mounted into a helium closed-cycle refrigerator for low-temperature measurements. Sample transfers for FANS measurements were performed in a helium-filled glove box (Lab master 130,

MBRAUN, Stratham, New Hampshire). Data were collected over the wavenumber range of  $200\text{ cm}^{-1}$  to  $1700\text{ cm}^{-1}$  at 4 K.

### Calculated Vibrational Spectra of Ibuprofen

First-principles calculations for a monoclinic crystal of ibuprofen were performed within the plane-wave implementation of the generalized gradient approximation to density functional theory (DFT) using the PWscf package. A Vanderbilt-type ultra-soft potential with Perdew-Burke-

**Fig. 3** Pore size distributions of porous media. **(a)**  $\text{SiO}_2$ ; **(b)** MAS.



Ernzerhof exchange correlation was applied (23). The dispersive interaction was corrected using a semi-empirical method (24). A cutoff energy of 544 eV and a  $(2 \times 4 \times 2)$  k-point mesh were found to be adequate for the total energy to converge within 0.5 meV/atom and 0.005 eV/Å. Structure optimizations were performed with respect to lattice parameters and atomic positions starting with the reported ibuprofen structure (25). The phonon calculations were then conducted with the DFT-optimized structure using the supercell method with finite displacements. Phonon spectra were also calculated for an isolated dimer and an isolated molecule of ibuprofen from optimized molecular configurations determined using a

$(30 \times 30 \times 30)$  supercell together with the molecular conformation found in the crystalline state as a reference.

## RESULTS AND DISCUSSION

Interactions between mesoporous adsorbents and adsorbates have long been an interest in both fundamental and applied research. The most prominent example is capillary condensation, with associated adsorption/desorption hysteresis, which is observed for a variety of molecules such as nitrogen, helium, water, or benzene. Despite the extensive

**Fig. 4** Small-angle X-ray scattering of mesoporous materials. (a)  $\text{SiO}_2$ ; (b) MAS.

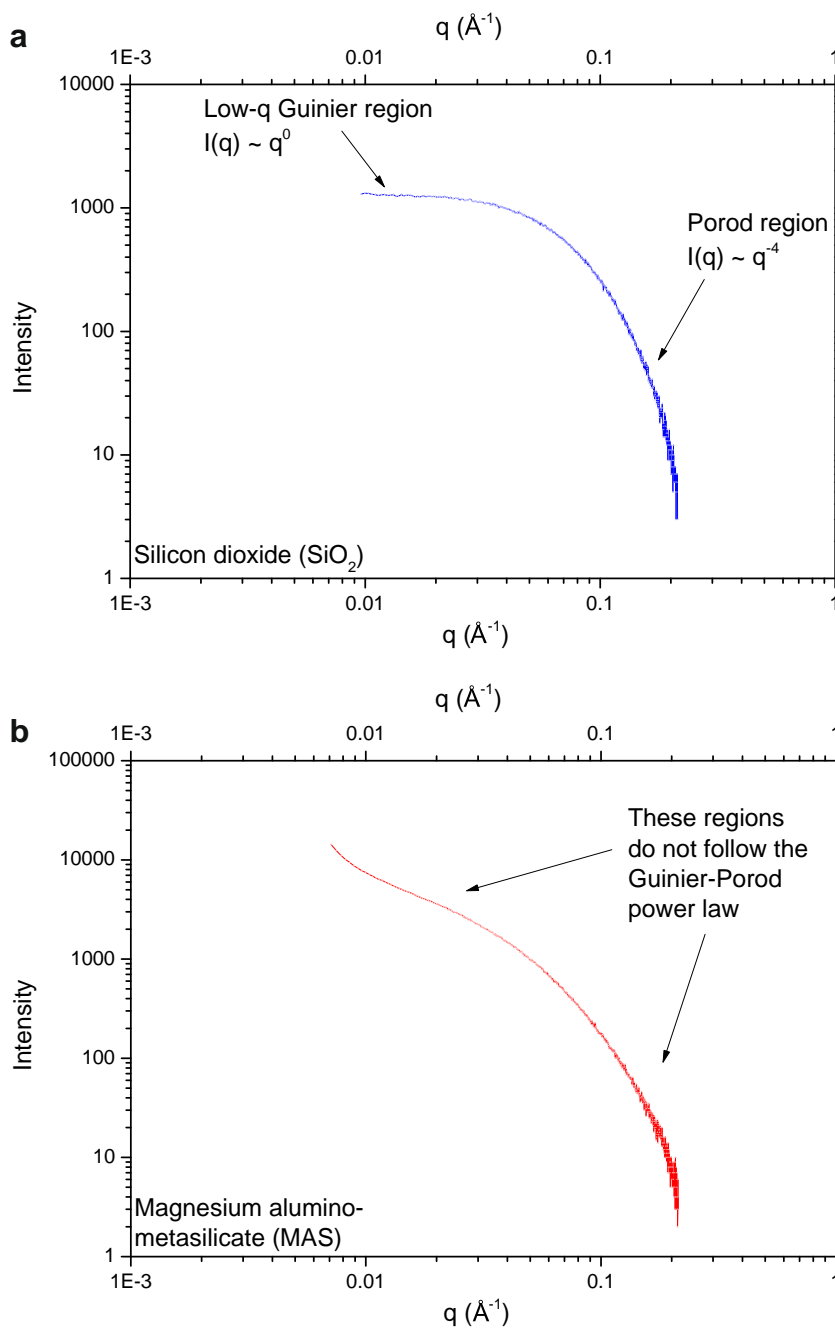
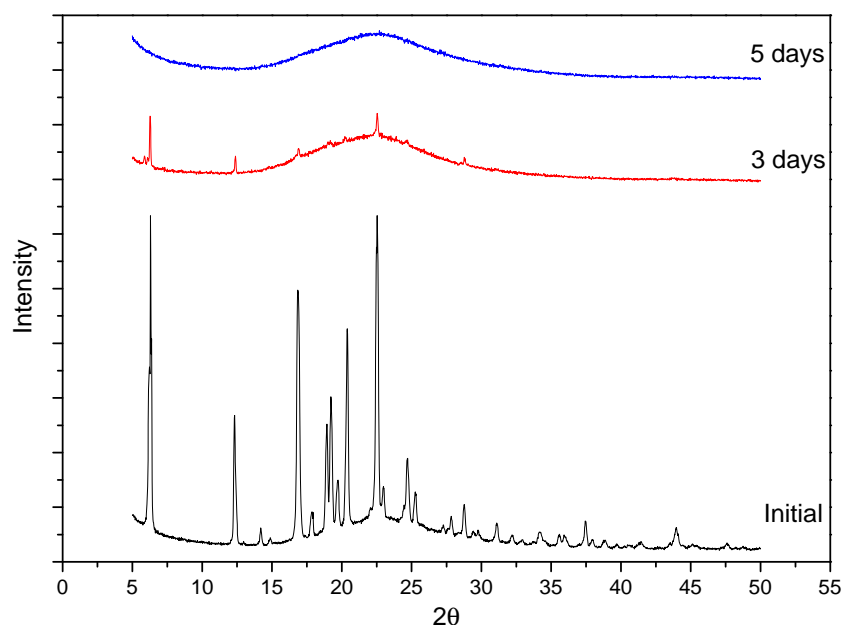


**Fig. 5** Powder X-ray diffraction patterns of a physical mixture of SiO<sub>2</sub> and ibuprofen stored at 40°C. X-ray patterns are offset for clarity.



work in this area, much less is known about the adsorption of medicinal compounds due to their complexity of chemical structures and the lack of suitable and sensitive techniques. As molecular interactions may hold the key to understanding and potentially predicting the properties and performances of pharmaceutical amorphous solids, their detailed understanding is critical to product development.

### Interaction of Ibuprofen with SiO<sub>2</sub> and MAS

Both SiO<sub>2</sub> and MAS are mesoporous, shown by the type IV isotherms with hysteresis loops (open symbols in Fig. 2) (26). The SiO<sub>2</sub> has a narrow pore size distribution (Fig. 3a). The shapes of its isotherms and the hysteresis loop (Fig. 2a), as well as the Guinier-Porod regions of the SAXS scan (Fig. 4a), indicate the material has isolated, cylindrical pores (26,27). However, the absence of Bragg peaks in SAXS scan suggests that these capillaries are randomly oriented. On the other hand, the MAS has irregular shaped pores with wider size distribution, as indicated by the nitrogen isotherms and SAXS scan (Figs. 2, 3 and 4).

The changes in crystallinity of ibuprofen in the powder mixtures were analyzed using PXRD. The X-ray patterns of the SiO<sub>2</sub>-ibuprofen mixture at a 3:1 mass ratio are shown in Fig. 5. The complete disappearance of the diffraction peaks

indicates phase transformation over time. These same observations were also made for the MAS-ibuprofen mixture. After the amorphization of ibuprofen, the amount of adsorbed nitrogen significantly decreased (solid symbols in Fig. 2). The volume occupied by ibuprofen was calculated assuming that it possesses the same density as neat ibuprofen (Eq. 1 in the Appendix). A reasonably good agreement between the reduction in the pore volume (column 4 of Table II) and the volume occupied by the adsorbed ibuprofen (0.42 cm<sup>3</sup>/g) suggests that the amorphized ibuprofen is incorporated within the pores of SiO<sub>2</sub> and MAS. While the macroscopic phase transformation was evident, the nano-scale arrangement of ibuprofen residing inside of the pores is of equal importance. How the molecules interact with the pore surfaces and among themselves can strongly influence the stability and performance of this amorphous drug delivery system, which is discussed below.

The molecular interactions of ibuprofen with both SiO<sub>2</sub> and MAS were examined using NVS. The spectra of neat crystalline ibuprofen and empty porous materials are shown in Fig. 6, normalized to the same mass and the number of incident neutron counts. Crystalline ibuprofen exhibits distinct phonon modes, while the bare porous materials show broad, diffuse phonon bands predominantly due to surface hydroxyl groups (Si-OH) and trapped sub-surface hydrogen.

**Table II** Changes in the Porous Properties of Silicon Dioxide (SiO<sub>2</sub>) and Magnesium Aluminometasilicate (MAS) Due to the Adsorption of Ibuprofen

Amorphous System	Total Pore Volume (cm <sup>3</sup> /g)			Specific Surface Area (m <sup>2</sup> /g)		Mean Pore Diameter (nm)	
	Initial	Final	Difference <sup>a</sup>	Initial	Final	Initial	Final
SiO <sub>2</sub> -Ibuprofen	0.87	0.39	0.48	517.7	239.9	5.8	4.3
MAS-Ibuprofen	1.2	0.82	0.38	321.4	180.9	15.5	12.4

<sup>a</sup>Obtained by (column 2 – column 3)

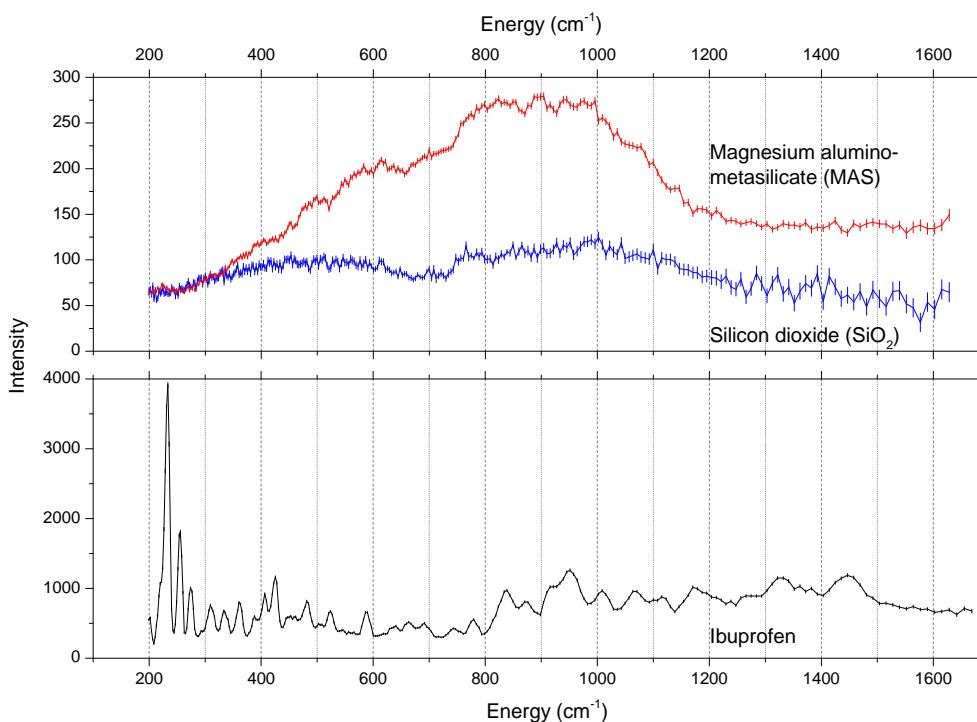
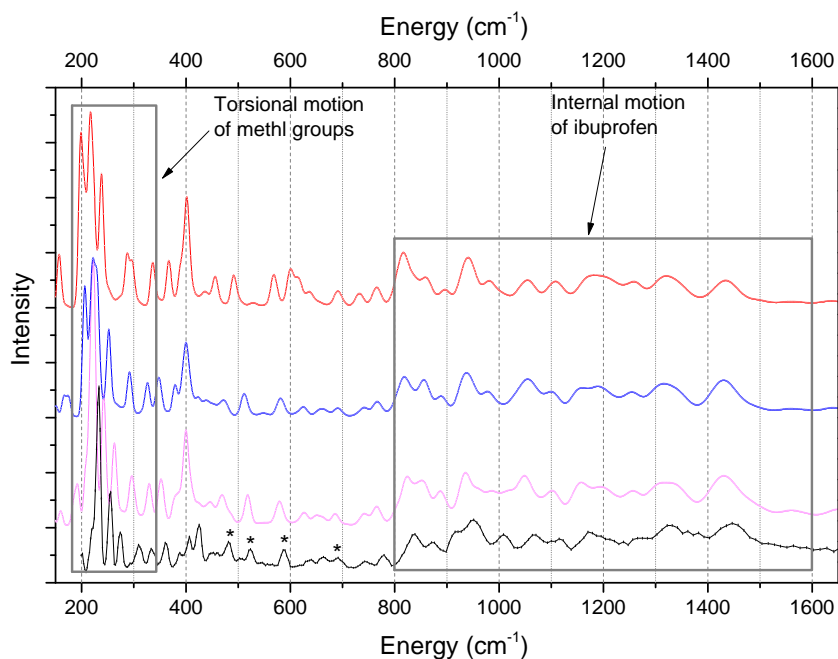


**Fig. 6** Neutron vibrational spectra of neat crystalline ibuprofen,  $\text{SiO}_2$  and MAS. The signals have been normalized to the same incident neutron counts and porous material:ibuprofen mass ratio of 3:1. Vertical error bars indicate one standard deviation.

In order to obtain the detailed description for normal-mode analysis, calculated phonon spectra of the crystalline compound, isolated dimer, and isolated molecule of ibuprofen were compared to the experimental spectra (Fig. 7). Aside from the expected minor peak shifts due to the shortcomings of DFT to describe the weak intermolecular interactions accurately, a good agreement overall is found between the

calculated and observed spectra of neat ibuprofen. Thus, the one-to-one correspondence between vibrational modes from calculation and experiment gives us confidence that first-principles calculations can be used to identify the origin of each observed vibrational feature. For example, the double hydrogen bond between the two  $-\text{COOH}$  groups is reflected in the O–H bending and C–OH stretching motions at

**Fig. 7** Calculated vibrational spectra of the isolated molecule (red), isolated dimer (blue), and crystalline compound of ibuprofen (magenta), compared with the experimental spectrum of neat crystalline ibuprofen (black). Vertical error bars indicate one standard deviation. Phonon bands related to the double hydrogen bonding involving  $-\text{COOH}$  and  $-\text{OH}$  motions are indicated by the star (\*) sign. Boxed regions represent the torsional motion of methyl groups and other internal motions of ibuprofen. Spectra are offset for clarity.





523  $\text{cm}^{-1}$  and 691  $\text{cm}^{-1}$ , respectively. The approximate descriptions of other phonon modes are summarized in Table III.

For the amorphous  $\text{SiO}_2$ -ibuprofen and MAS-ibuprofen systems, the spectra due solely to the adsorbed ibuprofen were obtained by subtracting the spectra of the empty porous materials after normalizing to the same mass of porous material (Fig. 8). With the incorporation of ibuprofen in the pores, several key differences can be observed. First, in the region between 440  $\text{cm}^{-1}$  and 800  $\text{cm}^{-1}$ , phonon bands due to the vibrational motions of the  $-\text{COOH}$  group become smeared compared to those of neat ibuprofen. The calculated spectra of both the isolated dimer and neat ibuprofen, which is also composed of dimers, display similar, distinct phonon bands due to dimer-related hydrogen bonding in this region. Hence, the smeared spectra of the amorphous systems in this region suggest that the confined ibuprofen molecules no longer exist as dimers. Otherwise, distinct phonon bands would still be present. It is likely that the ibuprofen  $-\text{COOH}$  groups preferentially interact with the pore surfaces, forming hydrogen bonds with the surface functional groups instead of with each other.

Second, in the lower-energy region between 200  $\text{cm}^{-1}$  and 320  $\text{cm}^{-1}$ , where the phonon bands are mainly due to the torsional motions of ibuprofen methyl groups, peaks exhibit significant smearing and broadening (Fig. 8). It is evident that these types of modes are sensitive to the environment, which is reflected in the changes in phonon bands as the molecules transition from the ordered crystal structure to a confined, disordered phase. On the other hand, the vibrational modes in the higher-energy region (800  $\text{cm}^{-1}$  to 1700  $\text{cm}^{-1}$ ), which are associated with internal modes such as  $-\text{CH}$  bending or deformation of the ring structure, appear to be insensitive to the environment, as they are largely unperturbed by the confinement. This is also corroborated by the first-principles calculations, where the calculated spectra above 800  $\text{cm}^{-1}$  are essentially the same for the isolated monomer, isolated dimer, and neat crystals (Fig. 7).

Hence, at the current drug loading, the experimental evidence points to a lack of ibuprofen dimerization within the  $\text{SiO}_2$  and MAS pores. The smearing of the phonon bands associated with the  $-\text{COOH}$  end of the molecule strongly suggests that ibuprofen forms hydrogen-bonding interactions with the surface functional groups on the pore wall. Therefore, a possible structural arrangement of the confined ibuprofen would involve either sub-monolayer or monolayer adsorption on the pore surfaces, which is further examined below.

### Structural Arrangements of Confined Ibuprofen

Since the observed NVS intensity is proportional to the hydrogen-weighted vibrational density of states, the integrated area under the curve (AUC) of a vibrational

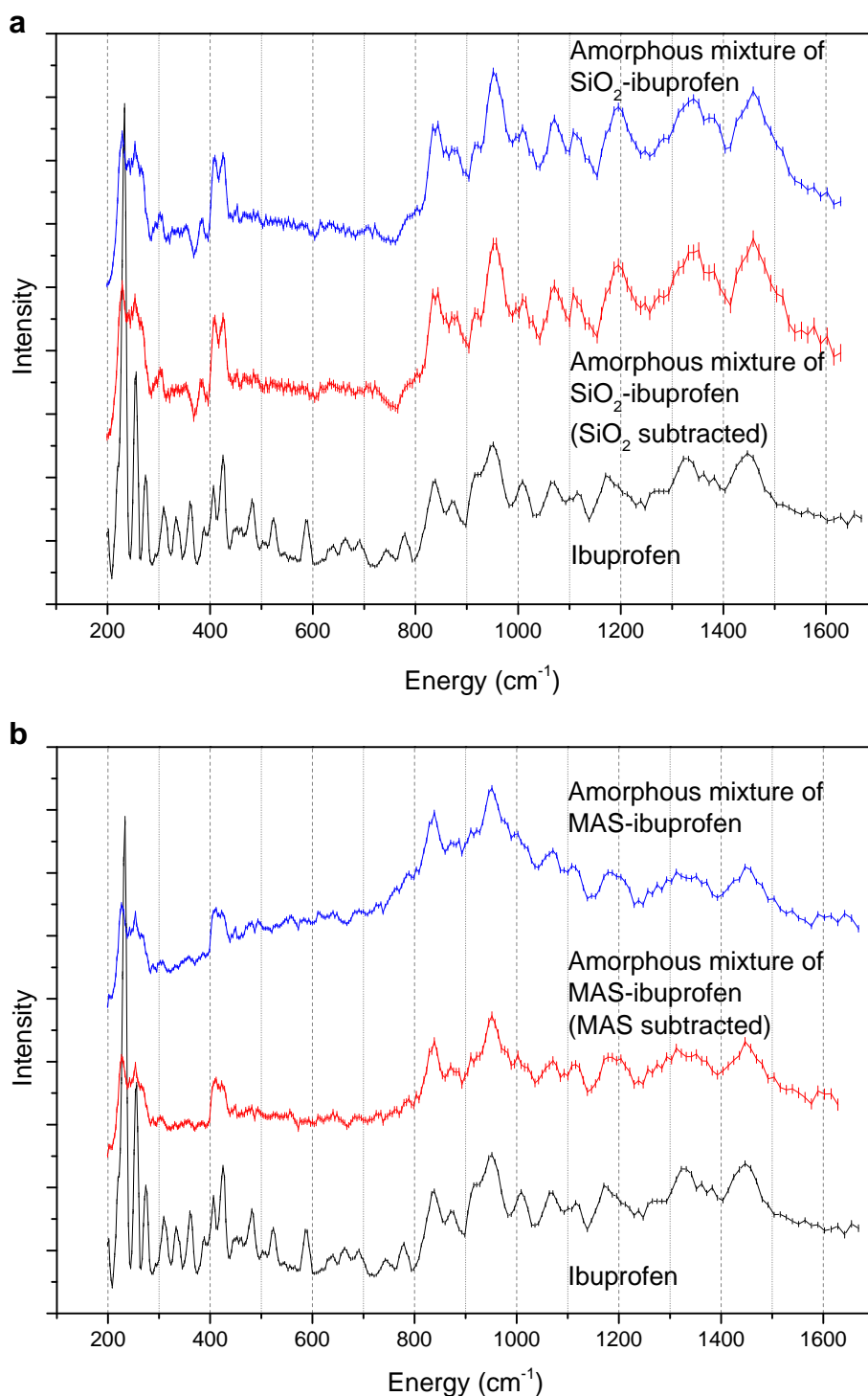
spectrum is, to a first approximation, proportional to the number of hydrogen atoms present in that sample. AUCs were determined for ibuprofen,  $\text{SiO}_2$ , and MAS samples (column 3 of Table IV). Assuming for the moment that the AUCs of the porous media are largely representative of hydrogen atoms from surface hydroxyl groups, and noting that each ibuprofen molecule possesses eighteen H atoms, the number of surface hydroxyl groups available per adsorbed ibuprofen molecule can be estimated from the ratio  $\text{AUC}_{\text{Si-OH}}:(\text{AUC}_{\text{Ibuprofen}}/18)$ . This ratio is 4.5 and 8.2 for  $\text{SiO}_2$  and MAS, respectively (column 4 of Table IV), which suggests that the number of surface hydroxyl groups far exceeds the ibuprofen molecules present at the current drug loading.

Additionally, as mentioned earlier, if a silica-based porous material is assumed to possess 4.6 hydroxyl groups/ $\text{nm}^2$ , this translates to 22  $\text{\AA}^2$ /hydroxyl group. The surface footprint of each ibuprofen, which has the  $-\text{COOH}$  end down, encompasses approximately 38  $\text{\AA}^2$ . Hence, by this independent calculation, approximately twice as many hydroxyl groups are necessary to accommodate a monolayer of ibuprofen molecules. The excess hydrogen estimated above from the AUC calculations suggests that half or more of the vibrational intensity from the empty  $\text{SiO}_2$  and MAS samples is due to phonon modes of trapped sub-surface H atoms. Since the iso-butyl group [ $-\text{CH}(\text{CH}_3)_2$ ] of ibuprofen would not be expected to participate in a hydrogen bond

**Table III** Approximate Description of Vibrational Motions of Ibuprofen Based on Density Functional Theory

Wavenumber ( $\text{cm}^{-1}$ )	Approximate Description of Motions
223	Torsional motion of $\text{C}^3-\text{C}^1\text{H}_3$ , $\text{C}^3-\text{C}^2\text{H}_3$ , and $\text{C}^{11}-\text{C}^{13}\text{H}_3$
255	Torsional motion of $\text{C}^3-\text{C}^1\text{H}_3$ , $\text{C}^3-\text{C}^2\text{H}_3$ , and $\text{C}^{11}-\text{C}^{13}\text{H}_3$
276	Bending motions of $\text{C}^4-\text{C}^3-\text{C}^1\text{H}_3$ , $\text{C}^4-\text{C}^3-\text{C}^2\text{H}_3$ , and $\text{C}^{11}-\text{C}^{13}$
336	Torsional motion of $\text{C}^3-\text{C}^1\text{H}_3$ , $\text{C}^3-\text{C}^2\text{H}_3$ , and $\text{C}^{11}-\text{C}^{13}\text{H}_3$
425	Benzene ring deformation
481	Rocking motion of $\text{C}^{11}-\text{C}^{12}-\text{OH}$
523	Bending mode of $\text{C}^{12}\text{O}-\text{H}$
589	Bending mode of $\text{C}^{11}-\text{C}^{12}-\text{OH}$
691	Stretching mode of $\text{C}^{12}-\text{OH}$
838	Benzene ring deformation
951	Bending modes of $\text{C}^6-\text{H}$ , $\text{C}^7-\text{H}$ , $\text{C}^9-\text{H}$ and $\text{C}^{10}-\text{H}$
1008	Bending mode of $\text{C}^{11}-\text{H}$
1063	Benzene ring deformation
1070	Rocking motion of $\text{C}^{11}-\text{C}^{13}\text{H}_3$
1331	Bending mode of $\text{C}^4-\text{H}$
1446	Bending mode of $\text{C}^4-\text{H}$

**Fig. 8** Neutron vibrational spectra of amorphous systems. **(a)** Amorphous  $\text{SiO}_2$ -ibuprofen mixture; **(b)** Amorphous MAS-ibuprofen mixture. Vertical error bars indicate one standard deviation. Spectra are offset for clarity.



surface interaction, a plausible structure would be a sub-monolayer to monolayer adsorption of ibuprofen on the surface, forming a close-packed arrangement (Fig. 9). This is also corroborated by the changes in surface areas and pore diameters. The reduction in surface areas was obtained from the nitrogen isotherm measurements (columns 5 and 6 of Table II). The total area of the  $-\text{COOH}$  groups in a 3:1 mass ratio mixture ( $366.1 \text{ m}^2$ ) translates into an approximate surface

coverage of 71 % on 1 g of  $\text{SiO}_2$  ( $517.7 \text{ m}^2/\text{g}$ ) and 114 % on 1 g of MAS ( $321.4 \text{ m}^2/\text{g}$ ), respectively (Eq. 2 in the Appendix). In the example of MAS-ibuprofen, although it is higher than 100 %, we believe that the adsorption of ibuprofen is likely at the transition of monolayer to multilayer coverage.

The changes in pore diameters suggest that the orientations of ibuprofen may be different in the two porous scaffolds. The decrease in pore diameter of MAS ( $31 \text{ \AA}$ )

**Table IV** Area Under the Curves (AUCs) of the Vibrational Spectra of Ibuprofen, Silicon Dioxide (SiO<sub>2</sub>) and Magnesium Aluminometasilicate (MAS)

Material	Mass (g)	Normalized AUC (cm <sup>-1</sup> /g)	AUC <sub>Porous material</sub> : (AUC <sub>Ibuprofen</sub> /18)
Ibuprofen	1.51	43476	–
SiO <sub>2</sub>	2.71	10815	4.5
MAS	4.84	19742	8.2

(columns 7 and 8 of Table II) agrees reasonably well with the total length of two ibuprofen molecules (23 Å), while the corresponding change in pore diameter of SiO<sub>2</sub> (15 Å) is somewhat less. It is possible that in the smaller pores of SiO<sub>2</sub>, the adsorption potential of the pore walls exerts stronger attraction to the adsorbed molecules than those in MAS. As a result, the molecules can be tilted closer towards the wall. On the other hand, the magnitude of the corresponding changes in pore diameter may merely reflect a reduced ibuprofen surface coverage on SiO<sub>2</sub> (71 %) compared to MAS (114 %), as calculated earlier, which would result in a smaller average change in pore diameter for the SiO<sub>2</sub> system. Nevertheless, the overall experimental evidence is consistent with the hypothesis that, at the current drug loading, most if not all ibuprofen molecules are adsorbed on the surface of the pores.

### Implications of Drug Under Confinement in Pharmaceutical Product Development

As ibuprofen molecules transition from ordered, crystal lattices to a disordered surface arrangement, what is the implication in the stability of a drug product over a pharmaceutically relevant

time scale, e.g., a 2-year shelf life? As medicinal compounds under confinement appear to be highly mobile (11,20), competing results in drug delivery can arise. On one hand, high mobility of drug molecules may favor faster drug release and better therapeutic effect; however, potential concerns about the kinetics of chemical degradation cannot be ignored (28–30). Future studies of molecular mobility, in reference to the chemical stability (31), of this amorphous drug delivery system would be helpful to address these questions.

In addition, the properties of the porous media can potentially play an important role as well. While SBA-15 and MCM-41 have been favored because of the ordered, hexagonal arrays of cylindrical pores, there is no conclusive evidence to suggest that they are better than the ones with a random structure, such as the SiO<sub>2</sub> and MAS used in the current investigation. Additional studies may shed further light on the effect of pore structure, and will aid in the design and improvement of porous excipients with optimal drug amorphization properties.

### CONCLUSIONS

In this paper, interactions between ibuprofen and mesoporous materials were studied using NVS and first-principles calculations. Experimental evidence shows that crystalline ibuprofen became amorphous once the molecules were incorporated into the nano-sized capillaries of SiO<sub>2</sub> and MAS. A comparison of the experimental data with first-principles calculations led us to conclude that the drug molecules failed to form dimers within the pores, adsorbing instead on the pore surfaces via hydrogen bonding between their –COOH groups and

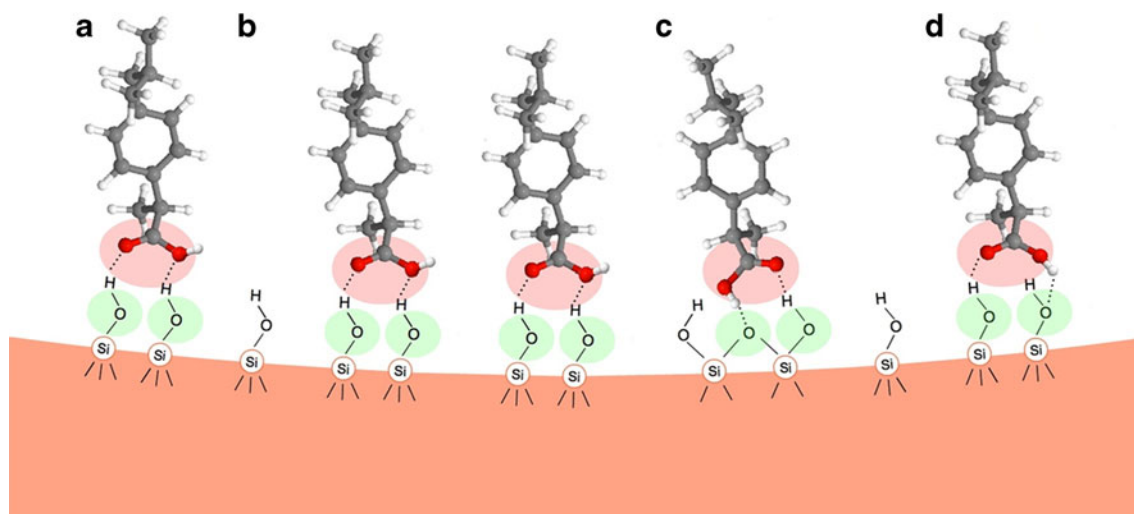


**Fig. 9** A schematic of the surface structural arrangements of ibuprofen in the pores of SiO<sub>2</sub>. Several possibilities of hydrogen bonding formation between the –COOH group of an ibuprofen molecule with either Si–OH or Si–O–Si are presented (not to scale). (a) Hydrogen bonding between –COOH of ibuprofen and Si–OH; (b) Unoccupied Si–OH group on the pore surfaces; (c) Hydrogen bonding between –COOH of ibuprofen and Si–O–Si; (d) Hydrogen bonding between –COOH of ibuprofen and Si–OH that is different than in (a).

the surface functional groups, resulting in sub-monolayer to monolayer coverage. This study has demonstrated that NVS can be a useful technique in characterizing the details of amorphous pharmaceutical systems.

Further investigation of this research is ongoing. For example, we plan to compare the vibrational spectra of neat amorphous ibuprofen prepared by melt quenching with those of the confined systems. Whether or not the inhibition of ibuprofen dimerization is solely due to confinement can be better addressed. In addition, we plan to measure vibrational spectra of amorphous systems with higher drug loadings, and a wider range of mean pore sizes for an expanded variety of porous materials to investigate their effects on stabilizing the

amorphous drugs in the pores. Understanding the mechanism of amorphization and interaction will be valuable for drug development. We anticipate that these scientific findings will contribute to the commercial utilization of stable amorphous drug delivery systems.

## ACKNOWLEDGMENTS AND DISCLOSURES

The authors acknowledge the helpful discussions with Dr. John J. Rush at NIST. This work utilized facilities supported in part by the National Science Foundation (NSF) under Agreement No. DMR-0944772. The National Research Council (NRC) Research Associateship Programs (RAP) is acknowledged for a postdoctoral fellowship to KKQ.

## APPENDIX

The volume occupied by the amorphized ibuprofen in the system:

$$\frac{0.33 \text{ g Ibuprofen}}{\text{g Porous material}} \times \frac{\text{mol}}{206.29 \text{ g}} \times \frac{6.022 \times 10^{23}}{1 \text{ mol}} \times (5 \times 7.6 \times 11.5) \times 10^{-24} \text{ cm}^3 = 0.42 \frac{\text{cm}^3}{\text{g Porous material}} \quad (1)$$

Total area covered by the carboxylic acid group (–COOH) of an ibuprofen molecule:

$$0.33 \text{ g Ibuprofen} \times \frac{\text{mol}}{206.29 \text{ g}} \times \frac{6.022 \times 10^{23}}{1 \text{ mol}} \times (5 \times 7.6) \times 10^{-20} \text{ m}^2 = 366.1 \text{ m}^2 \quad (2)$$

## REFERENCES

- Hancock BC, Zografi G. Characteristics and significance of the amorphous state in pharmaceutical systems. *J Pharm Sci.* 1997;86:1–12.
- Yu L. Amorphous pharmaceutical solids: preparation, characterization and stabilization. *Adv Drug Deliv Rev.* 2001;48:27–42.
- Sing KSW, Everett DH, Haul RAW, Moscou L, Pierotti RA, Rouquerol J, *et al.* Reporting physisorption data for gas/solid systems with special reference to the determination of surface area and porosity. *Pure Appl Chem.* 1985;57:603–19.
- Mellaerts R, Aerts CA, Humbeek JV, Augustijns P, Van den Mooter G, Martens JA. Enhanced release of itraconazole from ordered mesoporous SBA-15 silica materials. *Chem Commun.* 2007;1375–77.
- Qjan KK, Bogner RH. Application of mesoporous silicon dioxide and silicate in oral amorphous drug delivery systems. *J Pharm Sci.* 2012;101:444–63.
- Qjan KK, Bogner RH. Spontaneous crystalline-to-amorphous phase transformation of organic or medicinal compounds in the presence of porous media. Part 1: thermodynamics of spontaneous amorphization. *J Pharm Sci.* 2011;100:2801–15.
- Qjan KK, Suib SL, Bogner RH. Spontaneous crystalline-to-amorphous phase transformation of organic or medicinal compounds in the presence of porous media. Part 2: amorphization capacity and mechanisms of interaction. *J Pharm Sci.* 2011; 100:4674–86.
- Qjan KK, Wurster DE, Bogner RH. Spontaneous crystalline-to-amorphous phase transformation of organic or medicinal compounds in the presence of porous media. Part 3: effect of moisture. *Pharmaceutical Research* (In press, doi:10.1007/s11095-012-0734-4).
- Klafter J, Drake JM. *Molecular dynamics in restricted geometries.* New York: Wiley; 1989.
- Mellaerts R, Jammaer JAG, Van Speybroeck M, Chen H, Humbeek JV, Augustijns P, *et al.* Physical state of poorly water soluble therapeutic molecules loaded into SBA-15 ordered mesoporous silica carriers: a case study with itraconazole and ibuprofen. *Langmuir.* 2008;24:8651–9.
- Bras AR, Merino EG, Neves PD, Fonseca IM, Dionisio M, Schonhals A, *et al.* Amorphous ibuprofen confined in nanostructured silica materials: A dynamical approach. *J Phys Chem C.* 2011;115:4616–23.
- Iler RK. *The chemistry of silica.* New York: Wiley; 1979.
- Vansant EF, Van der Voort P, Vrancken KC. *Characterization and chemical modification of the silica surface.* Amsterdam: Elsevier; 1995.
- Zhuravlev LT. *The surface chemistry of amorphous silica.* Zhuravlev model. *Colloids Surf A Physicochem Eng Aspects.* 2000;173:1–38.
- Colthup NB, Daly LH, Wiberley SE. *Introduction to infrared and Raman spectroscopy.* Boston: Academic; 1990.
- Mitchell PCH. *Vibrational spectroscopy with neutrons with applications in chemistry, biology, material science and catalysis.* New Jersey: World Scientific; 2005.
- Willis BTM, Carlile CJ. *Experimental neutron scattering.* Oxford: Oxford University Press; 2009.

18. Certain trade names and company products are identified in this paper in order to specify adequately the experimental procedure. Such identification does not imply recommendation or endorsement by the National Institute of Standards and Technology, nor does it imply that the instruments, materials or suppliers identified are necessarily the best available for the purpose.
19. Perlovich GL, Kurkov SV, Hansen LK, Bauer-Brandl A. Thermodynamics of sublimation, crystal lattice energies, and crystal structures of racemates and enantiomers: Ibuprofen. *J Pharm Sci.* 2004;93:654–66.
20. Azais T, Tourne-Peteilh C, Aussenac F, Baccile N, Coelho C, Devoisselle J-M, *et al.* Solid-state NMR study of ibuprofen confined in MCM-41 material. *Chem Mater.* 2006;18:6382–90.
21. Barrett EP, Joyner LG, Halenda PP. The determination of pore volume and area distributions in porous substances. I. Computations from nitrogen isotherms. *J Am Chem Soc.* 1951;73:373–80.
22. Udovic TJ, Brown CM, Leao JB, Brand PC, Jiggetts RD, Zeitoun R, *et al.* The design of a bismuth-based auxiliary filter for the removal of spurious background scattering associated with filter-analyzer neutron spectrometers. *Nuclear Instruments and Methods in Physics Research Section A: Accelerators, Spectrometers, Detectors and Associated Equipment.* 2008;588:406–13.
23. Yildirim T. Structure and dynamics from combined neutron scattering and first-principles studies. *Chem Phys.* 2000;261:205–16.
24. Barone V, Casarin M, Forrer D, Pavone M, Sambri M, Vittadini A. Role and effective treatment of dispersive forces in materials: polyethylene and graphite crystals as test cases. *J Comput Chem.* 2009;30:934–9.
25. Shankland N, Wilson CC, Florence AJ, Cox PJ. Refinement of ibuprofen at 100K by single-crystal pulsed neutron diffraction. *Acta Crystallogr Sect C Cryst Struct Commun.* 1997;C53:951–4.
26. Gregg SJ, Sing KSW. Adsorption, surface area, and porosity. London: Academic; 1967.
27. Glatter O, Kratky O. Small angle X-ray scattering. London: Academic; 1982.
28. Hailu SA, Bogner RH. Effect of the pH grade of silicates on chemical stability of cocrystal amorphous quinapril hydrochloride and its stabilization using pH-modifiers. *J Pharm Sci.* 2009;98:3358–72.
29. Hailu SA, Bogner RH. Solid-state surface acidity and pH-stability profiles of amorphous quinapril hydrochloride and silicate formulations. *J Pharm Sci.* 2010;99:2786–99.
30. Hailu SA, Bogner RH. Complex effects of drug/silicate ratio, solid-state equivalent pH, and moisture on chemical stability of amorphous quinapril hydrochloride cocrystal with silicates. *J Pharm Sci.* 2011;100:1503–15.
31. Yoshioka S, Aso Y. Correlations between molecular mobility and chemical stability during storage of amorphous pharmaceuticals. *J Pharm Sci.* 2007;96:960–81.